Electronic supplementary information

Tuning photoelectron dynamic behavior of thiolate-protected MAu_{24} nanoclusters via heteroatom substitution

Xueke Yu,[a] Yuanze Sun,[a] Wen-wu Xu,[b] Junyu Fan,[c] Junfeng Gao,[a] Xue Jiang,[a] Yan Su,*[a] and Jijun Zhao[a]

[a.] *Key Laboratory of Materials Modification by Laser, Ion and Electron Beams (Dalian University of Technology), Ministry of Education, Dalian 116024, China.*

[b.] *Department of Physics, School of Physical Science and Technology (Ningbo University), Ningbo 315211, China*

[c.] *Department of Physics, (Taiyuan Normal University), Jinzhong 030619, China*

S1. NAMD computational methods

The time-domain nonadiabatic molecular dynamics (NAMD) simulation was performed with the Hefei-NAMD code[1] to investigate the excited-electron relaxation and e–h recombination dynamics in MAu_{24} (M = Pd, Pt, Cd, and Hg) nanoclusters. After the initial structure fully optimized at 0 K, the *ab initio* molecular dynamics (AIMD)[2] simulations were carried out to heat up the temperature of MAu_{24} nanoclusters to 300 K, in which the velocity scaling algorithm was adopted to achieve thermal equilibrium. Then, a 2 ps molecular dynamics simulation was performed in the microcanonical ensemble to generate the molecular dynamics trajectory with a 1 fs time step. Due to the strong coupling between higher energy states and LUMO+1 (process $e\tau$ in Fig. 3b) and the quantum decoherence effect is weak enough to be ignored, the process $e\tau$ was calculated by the fewest switches surface hopping (FSSH)[3,4] method. Moreover, the decoherence induced surface hopping (DISH)[5,6] method was adopted in the relaxation from LUMO+1 to LUMO and the e–h recombination process (processes & and ● in Fig. 3b), since these processes have larger bandgap and quantum decoherence effect. In all simulations mentioned above, the Brillouin zones were sampled by Γ point.

Table S1. The relaxation time (τ) and the vibrational modes coupled with the process ☞, &, and ● for MAu_{24} nanoclusters.

Systems	process ☞		process &		process ●	
	τ (fs)	vibrational modes (cm^{-1})	τ (ps)	vibrational modes (cm^{-1})	τ (ns)	vibrational modes (cm^{-1})
$PdAu_{24}$	190	50, 83, 116, 166, 217	250	33, 83	0.126	33
$PtAu_{24}$	380	50, 83, 133, 234	483	50	0.233	17, 67
$CdAu_{24}$	83	33, 100, 250, 517	86	17, 50, 117	8.03	50
$HgAu_{24}$	35	33, 117, 167, 217, 267, 400, 550	139	33, 67, 167, 217	7.55	50, 100

Table S2. The average NAC elements along 2 ps NAMD trajectory between different states from HE states to HOMO for excited-electron relaxation dynamics of $PdAu_{24}$ nanoclusters.

NAC (eV)	HOMO	LUMO	+1 (1)	+1 (2)	+2	+3	+4	+5	HE
HOMO	0.00	1.21	0.57	0.52	0.70	0.74	0.52	0.53	0.44
LUMO	1.21	0.00	1.32	1.12	0.80	0.71	0.73	0.67	0.66
+1 (1)	0.57	1.32	0.00	25.66	2.16	1.55	1.49	1.09	1.19
+1 (2)	0.52	1.12	25.66	0.00	2.81	2.01	1.72	1.44	1.20
+2	0.70	0.80	2.16	2.81	0.00	30.22	6.76	5.11	3.65
+3	0.74	0.71	1.55	2.01	30.22	0.00	24.70	7.97	5.93
+4	0.52	0.73	1.49	1.72	6.76	24.70	0.00	41.32	11.37
+5	0.53	0.67	1.09	1.44	5.11	7.97	41.32	0.00	45.08
HE	0.44	0.66	1.19	1.20	3.65	5.93	11.37	45.08	0.00

Table S3. The average NAC elements along 2 ps NAMD trajectory between different states from HE states to HOMO for excited-electron relaxation dynamics of $PtAu_{24}$ nanoclusters.

NAC (eV)	HOMO	LUMO	+1 (1)	+1 (2)	+2	+3	+4	+5	HE
HOMO	0.00	1.48	0.66	0.63	0.63	0.77	0.52	0.50	0.45
LUMO	1.48	0.00	0.85	1.42	0.73	0.88	0.89	0.58	0.50
+1 (1)	0.66	0.85	0.00	18.97	2.50	2.14	2.92	1.59	1.22
+1 (2)	0.63	1.42	18.97	0.00	5.79	2.19	1.85	1.71	1.59
+2	0.63	0.73	2.50	5.79	0.00	32.39	7.65	6.39	4.28
+3	0.77	0.88	2.14	2.19	32.39	0.00	33.21	8.67	6.76
+4	0.52	0.89	2.92	1.85	7.66	33.21	0.00	37.77	11.25
+5	0.50	0.58	1.59	1.71	6.39	8.67	37.77	0.00	50.96
HE	0.45	0.50	1.22	1.59	4.28	6.76	11.25	50.96	0.00

Table S4. The average NAC elements along 2 ps NAMD trajectory between different states from HE states to HOMO for excited-electron relaxation dynamics of $CdAu_{24}$ nanoclusters.

NAC (eV)	HOMO	L (1)	L (2)	+1	+2	+3	+4	+5	HE
HOMO	0.00	0.73	0.66	1.58	1.51	1.19	1.24	0.90	0.92
L (1)	0.73	0.00	16.74	1.96	1.58	1.32	1.38	1.05	1.00
L (2)	0.66	16.74	0.00	2.44	4.69	3.70	2.50	2.19	1.89
+1	1.58	1.96	2.44	0.00	25.57	4.69	3.70	2.50	2.19
+2	1.51	1.58	4.69	25.57	0.00	24.06	5.71	3.73	3.21
+3	1.19	1.32	3.70	4.69	24.06	0.00	28.02	6.80	4.20
+4	1.24	1.38	2.50	3.70	5.71	28.02	0.00	26.04	8.69
+5	0.90	1.05	2.19	2.50	3.73	6.80	26.04	0.00	43.38
HE	0.92	1.00	1.89	2.19	3.21	4.20	8.69	43.38	0.00

Table S5. The average NAC elements along 2 ps NAMD trajectory between different states from HE states to HOMO for excited-electron relaxation dynamics of $HgAu_{24}$ nanoclusters.

NAC (eV)	HOMO	L (1)	L (2)	+1	+2	+3	+4	+5	HE
HOMO	0.00	0.88	0.74	1.85	1.36	1.15	0.97	1.01	0.90
L (1)	0.88	0.00	14.98	2.10	1.43	1.12	1.06	1.21	1.00
L (2)	0.74	14.98	0.00	2.25	6.74	4.34	3.12	2.39	2.27
+1	1.85	2.10	2.25	0.00	24.84	6.74	4.34	3.12	2.39
+2	1.36	1.43	6.74	24.84	0.00	37.06	7.19	3.88	3.42
+3	1.15	1.12	4.34	6.74	37.06	0.00	32.99	6.77	4.67
+4	0.97	1.06	3.12	4.34	7.19	32.99	0.00	38.02	8.34
+5	1.01	1.21	2.39	3.12	3.88	6.77	38.02	0.00	36.97
HE	0.90	1.00	2.27	2.39	3.42	4.67	8.34	36.97	0.00

Table S6. Pure-dephasing (τ) along 2 ps NAMD trajectory between the LUMO+1 and HOMO for excited-electron relaxation dynamics of $PdAu_{24}$ nanoclusters.

τ (fs)	HOMO	LUMO	LUMO+1 (1)	LUMO+1 (2)
HOMO	0.00	3.13	6.31	5.90
LUMO	3.13	0.00	3.88	3.81
LUMO+1 (1)	6.31	3.88	0.00	10.17
LUMO+1 (2)	5.90	3.81	10.17	0.00

Table S7. Pure-dephasing (τ) along 2 ps NAMD trajectory between the LUMO+1 and HOMO for excited-electron relaxation dynamics of $PtAu_{24}$ nanoclusters.

τ (fs)	HOMO	LUMO	LUMO+1 (1)	LUMO+1 (2)
HOMO	0.00	6.38	5.11	6.84
LUMO	6.38	0.00	4.53	5.62
LUMO+1 (1)	5.11	4.53	0.00	9.88
LUMO+1 (2)	6.84	5.62	9.88	0.00

Table S8. Pure-dephasing (τ) along 2 ps NAMD trajectory between the LUMO+1 and HOMO for excited-electron relaxation dynamics of $CdAu_{24}$ nanoclusters.

τ (fs)	HOMO	LUMO (1)	LUMO (2)	LUMO+1
HOMO	0.00	6.51	6.43	6.55
LUMO (1)	6.51	0.00	11.11	7.57
LUMO (2)	6.43	11.11	0.00	7.81
LUMO+1	6.55	7.57	7.81	0.00

Table S9. Pure-dephasing (τ) along 2 ps NAMD trajectory between the LUMO+1 and HOMO for excited-electron relaxation dynamics of $HgAu_{24}$ nanoclusters.

τ (fs)	HOMO	LUMO (1)	LUMO (2)	LUMO+1
HOMO	0.00	8.56	9.58	5.05
LUMO (1)	8.56	0.00	14.14	5.11
LUMO (2)	9.58	14.14	0.00	5.21
LUMO+1	5.05	5.11	5.21	0.00

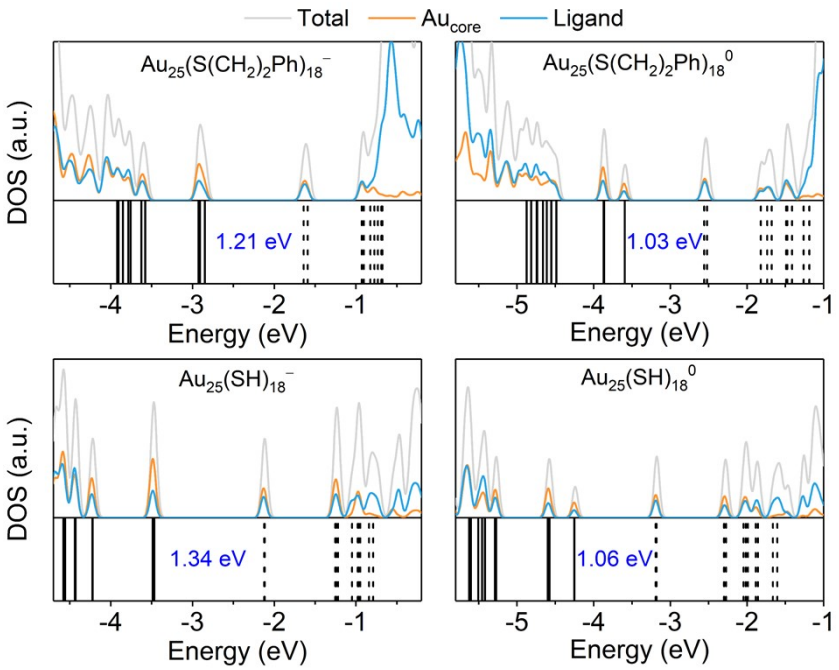

Fig. S1 Kohn–Sham orbitals (bottom panel) and density of states (top panel) of $Au_{25}(SR)_{18}^-$ (R = C_2H_4Ph and H) and $Au_{25}(SR)_{18}^0$ from DFT calculations. The HOMO-LUMO gaps are shown in blue values.

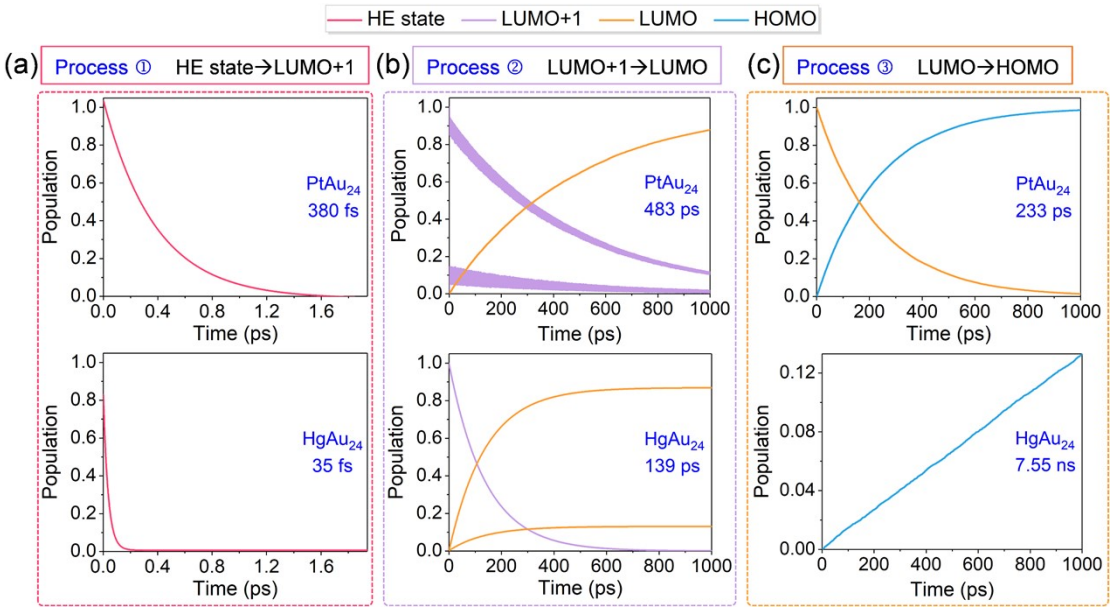

Fig. S2 Population evolution of energy states of $PtAu_{24}$ and $HgAu_{24}$ nanoclusters during three electron relaxation processes from HE states to HOMO. The three relaxation processes include ⟳ relaxation from higher–energy (HE) states to LUMO+1 (a), & relaxation from LUMO+1 to LUMO (b), ● *e*–*h* recombination between LUMO and HOMO (c).

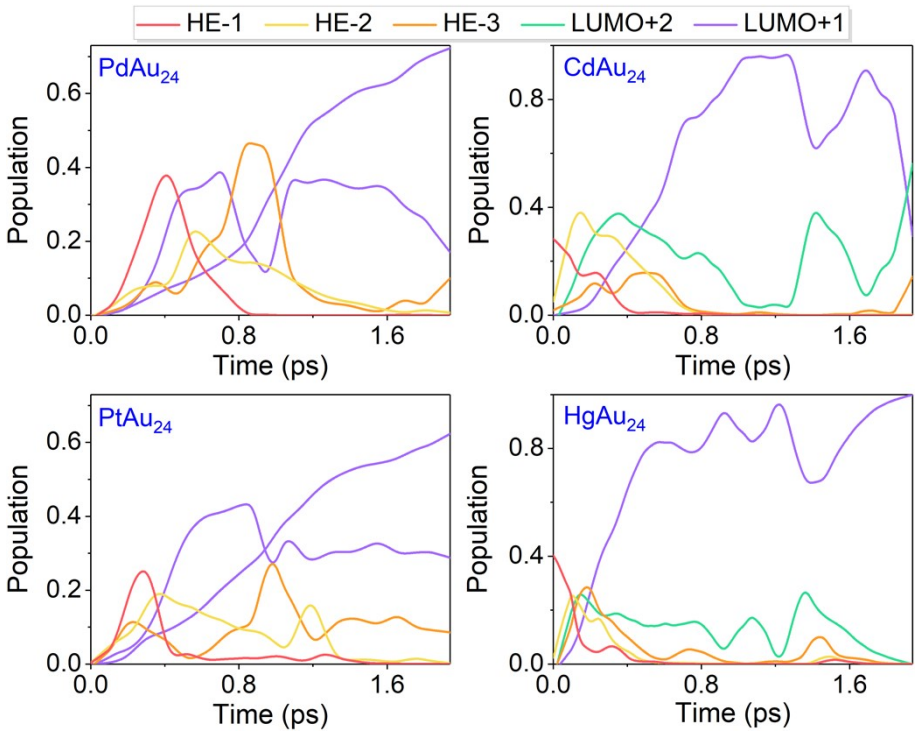

Fig. S3 The population evolution of relaxation states between HE–1 and LUMO+1 of MAu_{24} nanoclusters during the electron relaxation from HE states to LUMO+1.

Reference

1 Q. Zheng, W. Chu, C. Zhao, L. Zhang, H. Guo, Y. Wang, X. Jiang and J. Zhao, *WIREs Comput. Mol. Sci.*, 2019, **9**, e1411.

2 G. Kresse and J. Hafner, *Phys. Rev. B*, 1993, **47**, 558-561.

3 C. F. Craig, W. R. Duncan and O. V. Prezhdo, *Phys. Rev. Lett.*, 2005, **95**, 163001.

4 J. C. Tully, *J. Chem. Phys.*, 1990, **93**, 1061-1071.

5 H. M. Jaeger, S. Fischer and O. V. Prezhdo, *J. Chem. Phys.*, 2012, **137**, 22A545.

6 D. J. Trivedi and O. V. Prezhdo, *J. Phys. Chem. A*, 2015, **119**, 8846-8853.